

Available online at [www.sciencedirect.com](http://www.sciencedirect.com)

Chemical Engineering Research and Design

journal homepage: [www.elsevier.com/locate/cherd](http://www.elsevier.com/locate/cherd)ICChemE  
ADVANCING  
CHEMICAL  
ENGINEERING  
WORLDWIDE

# Bipolar membrane electrodialysis integration into the biotechnological production of itaconic acid: A proof-of-concept study

Tamás Rózsenberszki\*, Péter Komáromy, Éva Hülber-Beyer, Andrea Pesti, László Koók, Péter Bakonyi, Katalin Bélafi-Bakó, Nándor Nemestóthy

Research Group on Bioengineering, Membrane Technology and Energetics; Research Centre for Biochemical, Environmental and Chemical Engineering; Faculty of Engineering; University of Pannonia, Egyetem u. 10, 8200 Veszprém, Hungary

## ARTICLE INFO

### Article history:

Received 16 October 2022

Received in revised form

30 November 2022

Accepted 17 December 2022

Available online 21 December 2022

### Keywords:

Itaconic acid

Fermentation broth

Bipolar membrane

Electrodialysis

Crystallization

Fermentation temperature

Mass transfer mechanism

## ABSTRACT

Itaconic acid is a promising biobased organic acid that can be industrially produced in an eco-friendly way by aerobic fungal fermentation. It has many applications, e.g. in biopolymers, and has the potential to help replace or facilitate the green production of other similar but fossil-based chemicals. Nowadays, its production costs are still relatively high, partly due to the multistep product recovery process from the fermentation broth. In this study, a reduced number of downstream processes were evaluated to recover itaconic acid from model and real fermentation effluents. To the best of our knowledge, this is the first time the whole procedure is presented from the substrates to the solid and pure product, including fermentation, electrodialysis with bipolar membrane, evaporation and optimized crystallization. Based on the fermentation temperature and elevated pH, a synergistic effect was observed that intensified certain mass transfer mechanisms. Consequently, a significant amount of water (400 cm<sup>3</sup>) and itaconic acid (15 g) was transported into the alkaline concentrate. Moreover, novel outcomes about the condition, decolorization and process enhancements of the membrane (product recovery: 65–80 %, current efficiency: 42–76 %, product purity: 99 %) were recorded. Based on the results, our group is one step closer to the final concept of a continuously operated fermentation-electrodialysis integrated system.

© 2022 The Authors. Published by Elsevier Ltd on behalf of Institution of Chemical Engineers. This is an open access article under the CC BY license (<http://creativecommons.org/licenses/by/4.0/>).

## 1. Introduction

Itaconic acid or methylenesuccinic acid (C<sub>5</sub>H<sub>6</sub>O<sub>4</sub>) is a remarkable organic compound produced biologically by an aerobic filamentous fungus from carbohydrates (e.g. sugars, lignocellulosic biomass, etc.) (Komáromy et al., 2019; Saha, 2017). For instance, the detailed mechanisms regarding the biotechnological production of itaconic acid have been published (Kuenz and Krull, 2018). As a result of continuous

optimization, the biotechnological process is economical compared to the equivalent chemical synthesis (Bafana and Pandey, 2018).

Itaconic acid can be used in many fields such as synthetic resins, synthetic fibers, plastics, rubbers, surfactants and oil additives as well as in the polymer, textile, dental, ophthalmic and pharmaceutical drug delivery industries among others which have previously been described (Okabe et al., 2009). Additionally, a novel carboxyl functionalized biosorbent was made by grafting with itaconic acid on the seed composite for the purpose of removing metal ions (Mahour et al., 2022). Moreover, it can be used in super-absorbent polymer microspheres for the rapid concentration and quantification of viruses or other microbial waterborne

\* Corresponding author.

E-mail address:

[rozsenberszki.tamas@mk.uni-pannon.hu](mailto:rozsenberszki.tamas@mk.uni-pannon.hu) (T. Rózsenberszki).

<https://doi.org/10.1016/j.cherd.2022.12.023>

0263-8762/© 2022 The Authors. Published by Elsevier Ltd on behalf of Institution of Chemical Engineers. This is an open access article under the CC BY license (<http://creativecommons.org/licenses/by/4.0/>).

### Nomenclature

$A_M$	surface area of membrane ( $m^2$ ).
AEM	anion exchange membrane.
BM	bipolar membrane.
Cacid	segment/solution of the acidic concentrate.
Cbase	segment/solution of the alkaline concentrate.
CE	current efficiency.
CEM	cation exchange membrane.
E	specific energy consumption (kWh/kg product).
ED	electrodialysis.
EDBM	electrodialysis with bipolar membranes.
FERM-ED-IS	fermentation-electrodialysis integrated system.
I	current flowing through the membrane stack (A).
IA	itaconic acid.
ISPR	in situ product removal.
$m_{acid}^p$	mass of itaconic acid in the concentrate (g).
$m_{dil}^p$	mass of itaconic acid in the diluate (g).
PR	product recovery.
$R_M^s$	specific membrane resistance ( $\Omega m$ ).
U	Voltage across the membrane stack (V).
$\delta_M$	membrane thickness (m).
F	Faraday constant (96,500 C/mol).
$Em$	total transferred IA (mol).
$b$	ionic charge (2).
N	number of cell pairs.
t	operating time.

pathogens (Wu et al., 2020). Besides its wide range of applications, it is capable of replacing or supporting the sustainable synthesis of similar, albeit typically petroleum-based, chemicals (e.g. polyacrylic, acrylic and methacrylic acids) (El-Imam and Du, 2014; Erickson et al., 2012; Lansing et al., 2017; López-Garzón and Straathof, 2014; Okabe et al., 2009). Methacrylic acid (2-methylpropenoic acid, MAA) and methyl methacrylate (MMA) are important commodity monomers for the synthesis of numerous industrially significant plastics. The most significant petrochemical synthetic route to MAA/MMA is the acetone cyanohydrin process (ACH) (Nagai, 2001). Biobased MAA can be produced from simple sugars and citric acid via itaconic acid intermediate. Lansing et al. have summarized the existing synthetic routes to biobased methacrylic acid using IA (Lansing et al., 2017).

Over half of the total production costs of organic acids originate from the separation processes during manufacturing (Kim et al., 2022). The main limitations of IA market expansion are the relatively high production costs of \$1.6/kg (from glucose) and \$0.6/kg (from lignocellulosic feedstocks) as well as the high market price of \$1.80–2.00/kg (Bafana and Pandey, 2018; Nieder-Heitmann et al., 2018; Yang et al., 2020). If the price falls below approximately \$1.50/kg, the complete substitution of fossil-based polyacrylic acid with IA will have a market potential worth over \$11 billion annually (El-Imam and Du, 2014; Klement and Büchs, 2013). Alternatives exist to minimize the total cost, e.g. reducing the number of steps in downstream processes, fermentative production by genetically modified strains as well as the use of cheaper substrates, continuous fermentation and acid recovery. However, in the case of continuous fermentation, the

accumulation of the product or by-products can increase the likelihood of the inhibition effect occurring. According to other research groups, the production of IA already started to be inhibited above approximately 20–25 g IA/L (Eggert et al., 2019; Klement et al., 2012; Yahiro et al., 1995; Zambanini et al., 2017). In the light of this, although its accumulation should be avoided in the fermentation medium, the maximum product concentration is necessary for the efficient recovery of IA during the downstream steps.

For the aforementioned reasons, on the one hand, fermentation needs to be supported by another technique which is able to maintain the amount of the undesired compound at an adequate level in the fermentation broth (continuous in situ product removal, ISPR). On the other hand, a relatively pure and as concentrated as possible phase should result to facilitate the subsequent recovery stages such as crystallization. If each condition is met, the total cost could be reduced.

Several methods are available for the separation of the product from the fermentation broth, e.g. reactive extraction, crystallization, adsorption, precipitation and membrane processes (Gorden et al., 2017; Magalhães et al., 2017). According to Magalhães et al., despite the formation of by-products (waste salts), extraction and adsorption are remarkable techniques in terms of chemical-intensive processes because of the wide range of solvents, diluents and adsorbents required. Crystallization and membrane separation are energy-intensive low-emission processes. Direct crystallization as a result of evaporation is highly energy demanding. Techniques, namely adsorption, membrane bioreactors and reactive extraction, coupled with fermentation seem the most likely candidates for enhancing both the production yield and recovery efficiency.

The membrane separation techniques are applicable to other processes (e.g.: fermentation). Before the utilization of fermentation broth by membrane separation the only practical requirement is the pretreatment stage (suspended solid or mycelium removal) regarding to the continuous operation. One of the promising techniques for the separation of IA is electrodialysis (ED), an electromembrane process. ED is mostly used for the purpose of desalination due to the transfer of ions from the diluate to concentrate chambers through several pairs of perm-selective membranes containing monocharged (anion and cation exchange) functional groups across an electric potential (Strathmann, 2010). Organic acids can also be ionized and separated by ED (Handojo et al., 2019). Pal et al. demonstrated the advantages of integrating membrane-based techniques such as ED and electrodialysis with bipolar membranes (EDBM) into the industrial production of gluconic acid (Pal et al., 2016). The application of ED to fermentation is advantageous due to the preservation of the residual substrate in the diluate, which can be recirculated to be used in the fermentation process. Meanwhile, in continuous operations, the likelihood of product inhibition can be minimized by controlling the content of products or by-products. An ED membrane module can be equipped with bipolar membranes (EDBM). A bipolar membrane consists of two layers of membranes (both a cation and an anion exchange membrane), moreover, the dissociation of  $H_2O$  to  $H^+$  and  $OH^-$  takes place in the transition layer. With an appropriate combination of mono- and bipolar membranes, a free acid and base are formed from the salt without the addition of other chemical reagents (Sun et al., 2017). Furthermore, the protonated form of itaconic acid ( $H_2IA$ ) enables

efficient crystallization due to its lower solubility compared to the majority of itaconates at higher pHs (Gausmann et al., 2021). The deprotonated form of itaconic acid ( $IA^{2-}$ ) is preferable for the purpose of electrochemical separation thanks to the higher conductivity of the solution.

Our research aims to establish and develop the proof of concept regarding the continuous in situ product removal fermentation-electrodialysis integrated system (FERM-ED-IS) coupled with crystallization. This promising method could improve both the up- and downstream efficiencies simultaneously as a result of the higher production of IA and increased space-time yield. In the present work, model and real fermentation broths were separated by EDBM. Moreover, the effects of pH shifting, separating under elevated (35 °C) and room temperatures, recycling the diluate/product as well as optimizing the crystallization technique were investigated to get one step closer to a FERM-ED-IS concept.

## 2. Materials and methods

### 2.1. Fermentation broth materials

All of the chemicals used were described earlier in our previous papers (Komáromy et al., 2019; Rózsenszki et al., 2021). The majority of them were of analytical grade and utilized in the fermentation stage. The applied itaconic acid-producing microorganism was *Aspergillus terreus* NRRL 1960, a native itaconic acid overproducing strain isolated from soil in Texas. Two types of fermentation broths were used in this study. One of them originated from a batch process, while the other was collected from a long-term continuous process. The composition of the starting medium was identical in both cases using glucose as a source of carbon, as described by Komáromy et al. (Komáromy et al., 2019).

### 2.2. Fermentation broth preparation

The batchwise production of itaconic acid was performed in a 2 L Biostat fermentation system at 37 °C, 500 rpm and an aeration rate of 1 VVM. The pH was maintained at 3.0 with a 15 % w/w NaOH solution. The process was stopped after 7

days once no further itaconic acid had been produced over the previous 24 h.

Continuous fermentation was carried out in a LAMBDA MINIFOR bioreactor with an effective volume of 1.8 L. The operating temperature was 37 °C and the appropriate dissolved oxygen level was provided by pure oxygen gas at 0.2 VVM. The glucose concentration was maintained high (approximately 150 g/L). To effectively prevent microbial contamination, the pH was not controlled so it naturally reduced to below 2.5 and remained at that value throughout the fermentation.

Before electro dialysis, dead-end filtration was performed to remove the fungal biomass using a glass microfiber filter with a pore size of 1.2  $\mu\text{m}$  (55 g/m<sup>2</sup>; 270  $\mu\text{m}$  thickness). The clear solution obtained was tested on the electro dialysis unit directly or after appropriate pH adjustments had been made.

### 2.3. Electro dialysis with bipolar membranes

In this study, since a laboratory-scale P EDR-Z/4x multi-functional electro dialysis unit (manufactured by MemBrain) was used with the module variant of EDBM-Z/10–0.8 type, the electro dialysis unit was operated with ten membrane triplets (Ralex®) in the regular arrangement CEM-AEM-BM. The effective surface area of the membrane was 1984 cm<sup>2</sup>. A detailed description of the ED unit and the membranes used can be found in our previous papers (Rózsenszki et al., 2020, 2021). The module was cleaned by circulating HNO<sub>3</sub> (5 %) and NaOH (5 %) solutions according to the instructions described in the technical documentation.

Model and real fermentation broths were poured into a tank (diluate) with an IA content of between 28 and 33 g/L. Before the separation, all the fermentation broths were filtered as a pretreatment to avoid prompt fouling in the module caused by particles and the formation of mycelium from fungus. In some cases, the initial pH of the diluate was elevated by NaOH solution to study the shift in pH. Fig. 1 shows the schematic illustration of the system. The different segments are as follows: Diluate - initially this segment was filled with the feed solution; Cbase - this segment is between the CEM and BM; Cacid - this segment results in

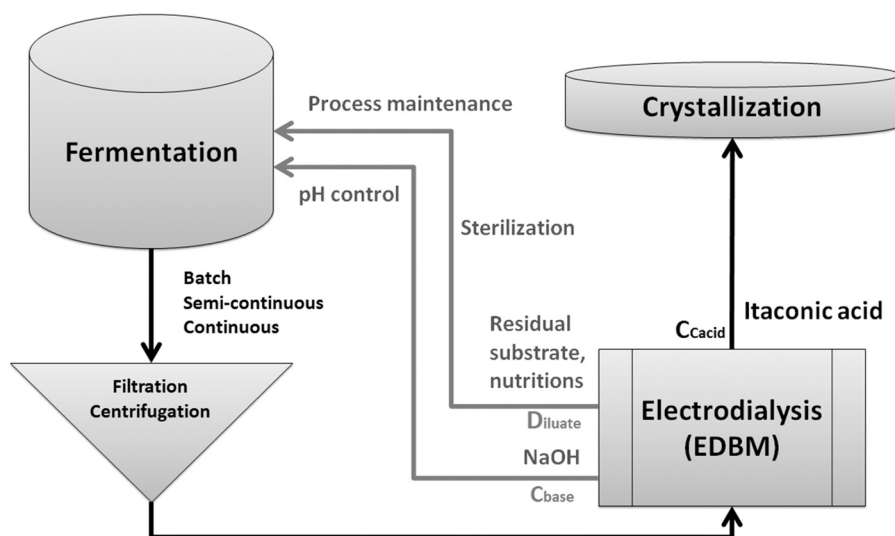


Fig. 1 – The schematic illustration of the IA separation and recovery from fermentation broth using three compartments EDBM coupled with crystallization. The recirculation of the side solutions (Cbase, Diluate) results low waste generation process.

the accumulation of the product between the membranes AEM and BM. Except one case, the separation tests were operated in batch mode for the better understanding of the transport mechanisms. In one case, semi-continuous operation was tested to determine the product accumulation in the Cacid. The elevated temperature of 35 °C (to simulate the fermentation conditions) was maintained by a water bath. During the electrodialysis, Na<sub>2</sub>SO<sub>4</sub> was used as the electrolyte solution (0.5 mol/L). In general, further chemicals are not required for the operation of the EDBM.

#### 2.4. Analysis

The concentration of IA was followed by a Young Lin Instrument Co., Ltd. high-performance liquid chromatography (HPLC) system (including a YL9109 vacuum degasser, a YL9110 quaternary pump and a YL9150 automatic sample dispenser) with a Hamilton PRP-X300 HPLC column 15 cm in length, 4.6 mm inner diameter, 5 μm particle size (Hamilton Company, Berkeley, CA, USA) and a YL9120 UV/VIS detector. Chromatographic conditions were as follows: 1 mM H<sub>2</sub>SO<sub>4</sub> and methyl alcohol as the eluents at a flow rate of 2.0 mL/min: 0–1 min 100 % of 1 mM H<sub>2</sub>SO<sub>4</sub>, 1–6 min increasing methyl alcohol ratio, 6–8 min until 100 % of 1 mM H<sub>2</sub>SO<sub>4</sub>. The injection volume was 100 μL, monitoring at 210 detection wavelength. The standard deviations were less than 5 %. The glucose content of the fluids was measured by 3,5-dinitrosalicylic acid (DNS) with a DR3900 Laboratory VIS Spectrophotometer (Lorenz, 1959). The electrical conductance of the fluids in the various segments of the EDBM unit was measured by a Radelkis OK-102/1 conductivity meter equipped with a Radelkis OK-9023 bell electrode using a cell constant of 0.97 cm<sup>-1</sup>. The data were collected online by LabVIEW software. The pH in each segment was monitored by a Radelkis OP-205/1 pH meter equipped with a WTW SenTix 60 pH electrode. The current was followed online by a Metrix MTX 3281 digital multimeter and evaluated by SX-DMM v 2.3 software. The elevated temperature of 35 °C (to imitate fermentation conditions) was provided by a water bath heated with a Sous Vide precision immersion circulator made by Ambiano in Germany.

#### 2.5. Crystallization

In this study, the acidic solution (Cacid) was concentrated by a rotary vacuum evaporator (Heidolph VV2000), the concentration of the solution was followed on an induction hotplate. The temperature of the solution was approximately 80 °C. The solution continued to be evaporated until the concentration of IA reached 250 g/L, which was estimated by the reduction in volume. After evaporation, the solutions were initially slowly cooled to room temperature and later to below 5 °C (in a fridge). The following day, the crystals were filtered from the solutions and the samples dried by a drying oven (Mettler UFE 400) at 105 °C. Recrystallization took place in a small volume of warm (80 °C) ion-exchanged water whilst continuously being stirred to dissolve the crystals of IA. The clear solution was once again cooled down and, once crystallized, the filtered crystals were dried according to the aforementioned method.

#### 2.6. Determination of specific membrane resistance

The specific membrane resistance ( $R_M^S$ ) was measured by DC chronopotentiometric polarization measurements. The

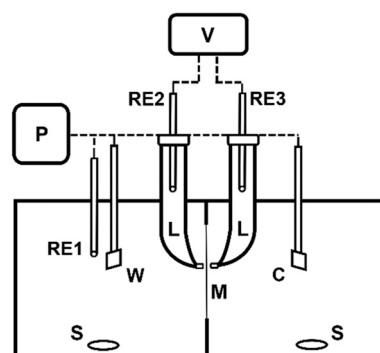


**Fig. 2 – Experimental setup for measuring the polarization of the membrane (C: Pt counter electrode; M: membrane under investigation; L: Luggin capillary with a porous frit; P: potentiostat; RE: Ag/AgCl reference electrode; S: magnetic stirrer; V: digital voltmeter; W: Pt working electrode).**

experimental setup (Fig. 2) consisted of a rectangular reactor divided into two chambers (each with a working volume of 160 mL) by the membrane under investigation. The membranes (M) were previously equilibrated with the test solution (0.5 M NaCl and real fermentation effluent containing 30 g/L of itaconic acid) by being soaked for at least 2 h. Pt plates with a surface area of 1 cm<sup>2</sup> and an Ag/AgCl (3M KCl, OP-0820 P, Radelkis, Hungary) electrode were used as working (W), counter (C) and reference (RE1) electrodes for chronopotentiometric control by a PalmSens3 potentiostat/galvanostat (P, PalmSens, The Netherlands). The current-density range between W and C was 6.25 – 75 A m<sup>-2</sup> (projected onto the surface area of the membrane). Two additional Ag/AgCl (3M KCl, OP-0820 P, Radelkis, Hungary) reference electrodes (RE2 and RE3) were inserted into Luggin capillaries (L) filled with 3M KCl, which were placed in the vicinity of both sides of the membrane surface via porous frits. The potential difference between RE2 and RE3 ( $U$ ) was recorded by a digital voltmeter (V, 34460 A, Keysight, USA). The electrolyte solution was stirred continuously by magnetic stirrers (S) during the experiments.

#### 2.7. Calculations

Based on the current ( $I$ ) and potential difference between the related electrodes, the resistance of the membrane+electrolyte ( $R_{M+E}$ ) was determined as the gradient of the  $I$ - $U$  data using Ohm's law. To obtain the pure membrane resistance ( $R_M^S$ ), the measurements were carried out in the absence of the membrane, thereby determining the electrolyte resistance ( $R_E$ ), which was then subtracted from  $R_{M+E}$ . The specific membrane resistance was then calculated by considering the thickness of the swollen membrane ( $\delta_M$ ) and its surface area ( $A_M = 4$  cm<sup>2</sup>) based on Eq. 1 (Geise et al., 2013):

$$R_M^S = R_M \cdot A_M / \delta_M \quad (1)$$

The current efficiency (CE) was calculated by Eq. (2):

$$CE(\%) = Em \cdot b \cdot F / \int Idt \cdot N \cdot 100 \quad (2)$$

where  $Em$  denotes the total amount of IA transferred in mol,  $b$  represents the ionic charge = 2,  $F$  stands for the Faraday constant = 96,500 A s/mol,  $N$  refers to the number of cell pairs,  $I$  equates to the current (A) and  $t$  is the operating time (Tran et al., 2015).

In this study, the percentages of the product (IA) and its recovery (PR) were calculated as follows:

$$PR(\%) = m_{acid}^p / m_{dil}^p * 100 \quad (3)$$

where  $m_{acid}^p$  denotes the mass of the product in the Cacid (g) in the permeate segment and  $m_{dil}^p$  stands for the mass of the product (g) in the fermentation broth that initially fed into the diluate segment before the separation commenced. It should be noted that using the mass (g) instead of concentration ( $g L^{-1}$ ) is more precise because in some special cases, as can be seen in the *Results and discussion* section, the concentration could be inaccurate due to the water transport effects during the process.

The specific energy consumption (E) of the electrodialysis was calculated by the following equation:

$$E = \int U \cdot I / m dt, kWh/kgIA \quad (4)$$

where  $U$  (V) denotes the potential difference across the membrane stack,  $I$  (A) represents the current through the whole stack and  $m$  (kg) stands for the total mass of IA, which migrated during the electrodialysis (Tongwen and Weihua, 2002).

### 3. Results and discussion

#### 3.1. Effect of the fermentation temperature on the electro-dialytic separation of IA

The biological production of IA is carried out industrially by aerobic fermentation caused by filamentous fungi. Generally, the most preferable productive species are the *Aspergillus terreus* strains and the optimal operating temperature is somewhere between 30 and 35 °C (Bafana and Pandey, 2018; Kuenz et al., 2012; Magalhães et al., 2019; Narisetty et al., 2021). During the strictly operated fermentation, the temperature and pH, among others, are the most critical parameters. In this section, to simulate a continuous fermentation-electrodialysis integrated system, an elevated fermentation temperature was applied during the separation of IA using aqueous model solutions. Table 1 includes the characteristics of the samples tested and the results after the separation. Each sample contained 33 g of IA and 33 g of glucose to simulate the residual substrate. The initial pHs were 3 and 5 since 7.4 (in the presence of the fully dissociated form of IA) had been tested in our previous works (Komáromy et al., 2020; Rózsensberszki et al., 2020, 2021).

As was expected, the shift in pH and the higher temperature increased the separation rate due to the facilitated ion transport caused by a higher ionic conductivity and current. However, the pH shifting reduced the CE due to the added charge used to move the ions. Moreover, a higher temperature (35 °C instead of 20 °C) coupled with pH shifting (from pH 3–5) increased the intensity of co-ion migration which intensified water transfer by electro-osmosis between the segments Cbase and Cacid. Co-ion migration transferred  $IA^{2-}$  from Cacid to Cbase (15 g of IA in Cbase) and the solvation shell (hydration shell) of the ions moved resulting in electro-osmosis and significant water transfer from Cacid to Cbase (+400  $cm^3$  of water in Cbase). The description of the mass transfer mechanisms in EDBM has been published by Wang et al. (2013), especially regarding IA separation with a similar EDBM configuration as can be seen in our previous work (Rózsensberszki et al., 2020; Wang et al., 2013). Based on

**Table 1 – IA recovery from aqueous model solutions by three-compartment EDBM at different initial pHs and temperatures.**

Operating parameters				
IA conc. in Diluate (g/L)	33	33	33	33
Glucose conc. in Diluate (g/L)	33	33	33	33
pH in Cbase, Cacid (Initial)	5	5	5	5
pH in Diluate (Initial)	3	3	5	5
Applied voltage (V)	20	20	20	20
Operating temperature (°C)	~20	35	~20	35
Operating time (hour)	5.5	4.5	4.5	4.0
<b>Results</b>				
<b>IA content (g/L, g)</b>				
Diluate	< 1, < 1	< 1, < 1	< 1, < 1	< 1, < 1
Cbase	4, 4	6, 6	7, 7	10, 15
Cacid	28, 28	27, 27	25, 25	23, 16
<b>pH in the segment</b>				
Diluate	4.3	4.0	4.2	4.5
Cbase	6.0	7.0	13.0	13.0
Cacid	3.6	3.0	3.0	3.0
<b>Efficiency (%)</b>				
current efficiency (CE)	99	99	75	50
product recovery (PR)	85	79	77	52
<b>Change in Volume during the operation (<math>\pm 10 cm^3</math>)*</b>				
Diluate	-60	-80	-140	-100
Cbase	+20	+30	+40	+400
Cacid	0	0	+20	-320

\* The net change in volume is negative (20–80  $cm^3$ ) predominantly due to the lack of sampling during HPLC as well as the solution in the tubes of the spectrophotometer and the ED equipment.

the results, it can be stated that separation at an elevated temperature with pH shifting in a solution of NaOH intensified co-ion migration. IA loss reduced PR and CE in the case of batch operations of 52 % and 50 %, respectively. Without adding extra ions to control the pH, CE was high at 99 % in both cases while PR was 85 % and 79 %, respectively. It would be interesting to investigate the impact of pH shifting at a particular fermentation temperature but a reduced applied potential. The latter parameter can lower the energy consumption as well as enhance CE and PR.

#### 3.2. IA separation by EDBM from real fermentation broths originating from batch fermentation

Unlike the previous test, in this case, a real fermentation broth was fed into EDBM equipment at room temperature. Table 2 includes the characteristics of the broth, the electro-dialytic conditions and the results regarding different initial pHs. It was shown that at room temperature and a higher pH (7.4 instead of 3 or 5) the impact on the IA content in Cbase (and the water transfer to Cbase) was less significant than when a temperature of under 35 °C was applied (see Table 1). According to the results, if the pH shifting of a diluate in a NaOH solution was avoided, the fermentation temperature did not cause a significant synergistic effect as described in the previous section. It seems that operating a fermentation-EDBM integrated system where the temperature and pH were elevated without modifying the applied potential could be disadvantageous in terms of the separation due to the intensified mass transfer mechanisms such

**Table 2 – IA recovery by EDBM from a real fermentation broth originating from a batch operation.**

Operating parameters		
Initial IA conc. in Diluate (g/L)		31
Applied potential (V)		20
Initial glucose conc. (g/L)		54.8
Parameters	Test 1	Test 2
Operating time (hour)	6.0	5.5
Operating temperature (°C)	~20	~20
Initial pH	3.0	7.4
<b>Results</b>		
Parameters	Test 1	Test 2
IA content in Diluate (g/L, g)	< 0.5, < 0.5	3, 3
IA content in Cbase (g/L, g)	6, 6	7, 8
IA content in Cacid (g/L, g)	25, 25	21, 20
pH in Diluate	4.0	9.5
pH in Cbase	13.0	13.7
pH in Cacid	2.2	2.6
CE (%)	74	42
PR (%)	80	65
<b>Glucose concentration (g/L)</b>		
Diluate	53.1	49.7
Cbase	0.3	0.3
Cacid	1.1	4.2
<b>Change in Volume during the operation ( ± 10 cm<sup>3</sup>)*</b>		
Diluate	-60	-100
Cbase	+20	+110
Cacid	+20	-30

\* The change in net volume is negative (20 cm<sup>3</sup>) predominantly due to the lack of sampling for HPLC as well as because of the solution in the tubes of the spectrophotometer and the ED equipment.

as co-ion migration. Without elevating the pH, 74 % and 80 % of PR and CE were achieved, respectively, which are higher than in the case of a pH-shifted fermentation broth where 42 % and 65 % of PR and CE were calculated, respectively.

### 3.3. Evaluation of membrane ageing and resistance in a model electrolyte and real fermentation effluent

Ion exchange membranes with high ionic conductivity (i.e. low ion transport resistance) are vital for ensuring an efficient ED process. Moreover, when a membrane stack consisting of a series of membranes is used, the individual membrane resistances could significantly contribute towards the overall resistance of the system.

During the separation process, it could be observed that IA can pass through the membranes not only into Cacid but into Cbase as well. Since this phenomenon may lead to a reduction in PR, monopolar membranes used in the stack were tested by DC chronopotentiometric polarization to investigate membrane ageing by evaluating the specific membrane resistance of the IEMs. The total operating time of IEMs was ~200 h at the time of the experiments, during which model and prefiltered fermentation broths containing IA, glucose, malic acid and other by-products were separated via ED. In some cases, extreme pH values were applied (e.g. pH =1.5, 13.5), which could potentially have contributed to membrane ageing. Although a membrane cleaning procedure was carried out twice a month, separation of the fermentation broth – which may contain microbes and residual substrates – further increases membrane stress and the risk of membrane fouling during excessively long operating



**Fig. 3 – Bipolar (BM), Cation exchange (CEM) and Anion exchange (AEM) membranes after a total operating time of 200 h. IA containing model solutions and filtered real fermentation broths were used in the membrane stack.**

times. Indeed, contamination could be observed on the membrane surface, mainly in the case of AEM (Fig. 3):

Firstly, the specific membrane resistance was characterized for reference purposes in a standard electrolyte solution (0.5 M NaCl). For both membranes tested,  $R_M^S$  fell within the range of 35 – 45  $\Omega$  cm. The CEM exhibited a higher  $R_M^S$  of 44.5  $\Omega$  cm, while the AEM had somewhat of a lower resistance ( $R_M^S = 36.2 \Omega$  cm). Although the specific resistances of tested membranes previously operated for approximately 200 h in the treatment model and real itaconic acid-containing effluents remained low ( $R_M^S < 120 \Omega$  cm in 0.5 M NaCl as assured by the manufacturer), the results did not indicate the presence of severe membrane fouling, since the deposition of the foulant on the membrane surface or ion-exchange functional groups would lead to an obvious decrease in  $R_M^S$  (Mikhaylin and Bazinet, 2016). In some cases, even though the test solution (NaCl) could promote the detachment of the foulant from the membrane surface (Mikhaylin and Bazinet, 2016), no detached particles were visible in the electrolyte after measurements had been taken. Nevertheless, in order to address the potential detachment and gain information about  $R_M^S$  in the actual separation media, measurements using a real fermentation effluent (of which the electrolytic conductivity was 8.8 times lower than that of 0.5 M NaCl) were taken. The results showed that the CEM exhibited the lower resistance (100.8  $\Omega$  cm), while  $R_M^S = 114.5 \Omega$  cm was obtained for the AEM. Similarly to the NaCl tests, the data suggested that no severe fouling layer formed on the membrane surface (the measured resistances remained lower than the upper limit according to the manufacturer, although the conductivity of the real effluent was significantly lower compared to that of 0.5 M NaCl). Based on these observations, it can be assumed that certain colorants became trapped in the structure of the AEM membrane (see Fig. 3) which did not significantly affect its properties.

During the ED operation, the BM was not in direct contact with the fermentation broth. Besides determining key elements that contributed to its resistance, it may also be appropriate to periodically monitor the specific membrane resistance during an ED operation for the purpose of evaluating membrane ageing and the phenomenon of membrane fouling, thereby initiating the cleaning or replacement of the membrane. Although this study mainly focuses on the separation and recovery of IA from the fermentation broth, further tests would be useful to monitor the resistance of the membranes, including BMs, during separation.

### 3.4. IA separation by EDBM with a modified membrane stack from a fermentation broth originating from continuous fermentation

There are parameters such as the applied potential/current, flow rate of the segments or the total effective surface area of the membrane module that can affect on the separation intensity. In the following test, the membrane module was modified to analyze the process when the current density was raised without increasing the applied potential. Reduced numbers of membranes were applied, namely 6 pieces of CEM instead of 11, 5 pieces of AEM instead of 10 and 5 pieces of BM instead of 10. The total effective surface area of the membrane was 1024 cm<sup>2</sup> instead of 1984 cm<sup>2</sup>.

The results are summarized in Table 3, which show that the modified module ensured a higher current density (182 A/m<sup>2</sup>) compared to the previously discussed tests (see Table 5). The reduction in the number of membranes lowered the internal resistance of the membrane stack. The current was higher than in the tests described in the Sections 3.1, 3.2. The driving force of the separation process intensified (faster ion transport shortened the operating time to 3.8 h instead of 5.6 or 6.0, moreover, this modification resulted in a similar PR of 71.4 %) but a higher CE of 76.2 % instead of 42 % was reported in a previous study, where a similar broth and the same ED equipment without modification of the module were used. Only a moderate level of water transfer from the Cacid segment is observed compared to the phenomena described in the section where the effect of the mesophilic temperature was tested.

### 3.5. Simulation of a continuously operated separation with a sequential batch model fermentation broth

To simulate the behavior of EDBM in terms of the continuous operation, the dose of the model fermentation broth tested

**Table 3 – IA separation by EDBM from a pH-shifted fermentation broth (continuous fermentation) with a modified membrane module.**

Operating parameters	
Initial IA content in Diluate (g/L; g)	27.8; 25.6
Initial pH	7.4
Applied potential (V)	20
Initial glucose conc. (g/L)	122
Operating time (hour)	3.8
<b>Results</b>	
IA content in Diluate (g/L; g)	3.0; 2.3
IA content in Cbase (g/L; g)	3.6; 4.0
IA content in Cacid (g/L; g)	31.5; 18.3
pH in Diluate	10.2
pH in Cbase	13.3
pH in Cacid	2.0
CE (%)	76
PR (%)	71
<b>Glucose concentration (g/L)</b>	
Diluate	108
Cbase	1.3
Cacid	7.7
<b>Change in Volume during the operation ( ± 10 cm<sup>3</sup>)*</b>	
Diluate	-120
Cbase	+180
Cacid	-80

\* The change in net volume is negative (20 cm<sup>3</sup>) predominantly due to the lack of sampling for HPLC as well as the solution in the tubes of the spectrophotometer and the ED equipment.

**Table 4 – Results of an IA separation consisting of two feedings using a model fermentation broth.**

Operating parameters		
Model fermentation broth to Diluate	First feeding	Second feeding
Initial IA content in Diluate (g/L; g)	30.2; 30.2	29.4; 29.4
Initial pH	5.0	5.0
Applied potential (V)	20	
Initial glucose conc. (g/L)	92	92
Operating time (hour)	4	4
<b>Results</b>		
	First feeding	Second feeding
IA content in Diluate (g/L; g)	0.003; 0.003	0.003; 0.003
IA content in Cbase (g/L; g)	1.95; 2.85	9.05; 15.02
IA content in Cacid (g/L; g)	27.6; 22.1	67.4; 45.8
pH in Diluate	3.3	3.6
pH in Cbase	12.6	12.7
pH in Cacid	1.2	1.2
CE (%)	71.4	
PR (%)*	72.6	
<b>Glucose concentration (g/L)</b>		
Diluate	170.0	
Cbase	1.3	
Cacid	9.2	
<b>Change in Volume during the operation ( ± 10 cm<sup>3</sup>)</b>		
Diluate	-120	-120
Cbase	+400	+200
Cacid	-280	-120

\* The change in net volume is negative (0–40 cm<sup>3</sup>) predominantly due to the lack of sampling for HPLC as well as the solution in the tubes of the spectrophotometer and the ED equipment.

was doubled. Table 4 summarizes the details and main results of the test. The configuration of the EDBM apparatus was the same as in the previous test (modified module was used). The separation of the first feed resulted in a lower IA content in Cbase (seen in Fig. 4.) compared to the results regarding the separation of the second feed. As was expected, due to the higher current density in the second part of the separation, co-ion migration intensified increasing the rate of IA movement to Cbase (15.0 g of IA instead of 2.9 g).

Meanwhile, unexpectedly less water transfer was observed, which is interesting because higher current densities favor electroosmosis which should enhance the rate of water

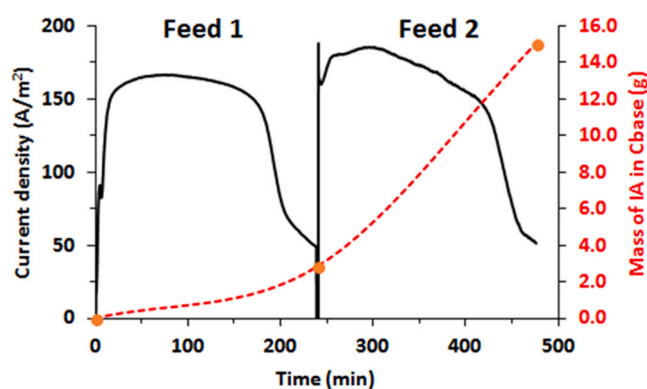


**Fig. 4 – Demonstration of double feeded EDBM process under fixed applied potential. Orange points: mass of IA in the segment of Cbase. Black line: Current density during the operation.**

transfer. Probably, in this case, the osmotic force acted in the opposite direction due to the concentration gradient between the segments and moderate level of water transfer was observed from Cacid into Cbase. Water transfer from Cacid into Cbase concentrated the IA in Cacid which could be beneficial with regard to crystallization. However, the leakage of IA from Cacid to Cbase should be avoided to enhance product recovery. Based on the results, it would seem that during a continuous long-term EDBM operation, the applied potential should be maintained at an adequate level to minimize the phenomena caused by high current densities. Therefore, electro-generated phenomena such as co-ion migration can be minimized and PR enhanced. The overall PR and CE were 72.6 % and 71.4 %, respectively. A moderate applied potential, especially during the second separation of the feed, probably resulted in a higher PR and CE.

### 3.6. Summary of the main separation results regarding the different fermentation broths treated by EDBM

In Table 5, the main results are summarized and compared to our previous tests because of the limited number of studies in the literature regarding IA separation by EDBM using real fermentation broths. PR reached between 65 % and 77 % regarding fermentation broths at elevated initial pHs. Without pH shifting, these values were between 74 % and 80 %. In the case of CE, pH shifting reduced these figures to between 41 % and 42 %. Since the membrane stack contains a reduced number of membranes, CE could be improved by 34–35 %, that is, from 41 % to 76 %, compared to similar tests where a fermentation broth was pH shifted. Additionally, although these results were higher than those from tests in the absence of pH shifting (63 % and 74 %), more energy was required (2.6 kWh/kg IA).

Szczygielka et al. used EDBM to recover succinic acid (SA,  $C_4H_6O_4$ ) from a three-component model solution containing 43 g/L succinic acid, 42 g/L glycerol and 20 g/L lactose (Szczygielka et al., 2017). Based on their results, at a current density of 120 A/m<sup>2</sup>, 31 g/L of SA was separated from the model solution. Furthermore, the energy consumption and

current efficiency were equal to 3.2 kWh/kg and approximately 31 %, respectively. The authors tested the actual post-fermentation broth and recovered 20.2 g SA/L. By comparing it with experimental data obtained for the EDBM of model solutions, a decrease of approximately 35 % in the concentration of succinate ions through the AEM was observed due to the complex composition of the fermentation broth.

### 3.7. Recovery of IA from the Cacid segment by crystallization after EDBM separation

Typically, IA produced by fermentation is purified by filtration and multistep concentration by evaporating water with the subsequent crystallization below a pH of 3.84 (Regestein et al., 2018). Even though Dwiarti et al. obtained highly pure IA (97.2–99.0 %), the PR was only 51 % due to the loss of the product as a result of the multistep crystallization (Dwiarti et al., 2007). According to Okabe et al., the classical process without EDBM is usually characterized by large thermal energy demands due to the evaporation stage and low levels of purity of products within the cooling crystallization step (Okabe et al., 2009). Furthermore, the latter stage makes further purification steps such as secondary crystallization, recrystallization and decolorization by treatment with activated carbon at 80 °C necessary to produce high-quality IA.

By integrating EDBM into IA separation, the filtration of insoluble particles such as microorganisms is necessary but the retention of colorants as well as parts of ionic and other non-ionic compounds such as residual substrates to be recirculated into the fermentation process can be provided (Rózsensberszki et al., 2021). It should be noted that the recirculation of the diluate back into the fermentation stage requires further investigation, e.g. evaluation of the biocompatibility of the fungal activity during the fermentation. In addition, a continuous operation is beneficial to increase the concentration of IA in the Cacid solution before crystallization and decrease the number of crystallization steps. As is clearly illustrated in Fig. 5 during the continuous fermentation process by *Aspergillus terreus*, smaller amounts of colorants as by-products were formed. The presence of less

**Table 5 – Summary and comparison of the main results regarding IA separation under similar EDBM conditions.**

Feed solution (operation method)	Initial pH	CE (%)	PR (%)	Current density (A/m <sup>2</sup> )	Energy consumption of ED process (kWh/kg IA)	Remarks	References
fermentation broth (semi-continuous)	3.0	63	74	53	1.5	–	Rózsensberszki et al., 2021
fermentation broth (semi-continuous)	7.4*	41	77	94	2.2	–	
fermentation broth (batch)	3.0	74	80	44	1.1	EDBM followed by crystallisation	present study
fermentation broth (batch)	7.4*	42	65	67	2.0	EDBM followed by crystallisation	present study
fermentation broth (continuous)	7.4*	76	71	182	2.6	Effective surface area of membrane module reduced, EDBM followed by crystallisation	present study
model fermentation broth	5.0	71	73	166; 185**	2.3	reduced effective surface area of membrane, refeeding: double the dose of feed solution (diluate), EDBM followed by crystallisation	present study

\*\*first feed; second feed

\* initial pH of fermented broth was shifted by NaOH solution



**Fig. 5 – Comparison of the coloring effect between the batch (1.) and continuous (2.) IA fermentations from glucose using the *Aspergillus terreus* strain.**



**Fig. 6 – Itaconic acid crystals recovered from fermentation broths by EDBM following different crystallization procedures - A: Crystallization without stirring and drying at 105 °C, B: Crystallization with stirring and drying at 105 °C, C: Crystallization with stirring and multistep drying at 60 °C, 80 °C and 105 °C.**

colorant is beneficial for the following recovery process to produce highly pure IA. Although the early results seem promising, further tests are required to identify the reasons why less colorant as a by-product was formed during the fermentation.

In this study, IA separation using EDBM from model and real fermentation broths was followed by crystallization (see Table 5). During the separation by EDBM, a significant amount of the colorants in the fermentation broth can be retained in the diluate (Rózsenszki et al., 2021). However, due to the high substrate (glucose) concentration gradient between the Cacid segment and the diluate, a small proportion of it can be transferred into the Cacid segment (Tables 2–4). During evaporation and crystallization, although the presence of these impurities can cause coloration, an adequate level of crystallization in addition to washing and stirring coupled with a multistep heating technique can significantly reduce the degree of aforementioned contamination, as can be seen in Fig. 6:

Based on the experiments, stirring during the slow crystallization process was necessary to prevent the colorants, residual substrates or other impurities from becoming trapped inside the crystals formed. The accumulated impurities in the supernatant can be removed and the process followed by washing then drying. Since gradual heating resulted in efficient drying, the trace residues could not be caramelized on the surface of the crystals. Therefore, by

applying this technique, that is, continuous, slow stirring during crystallization and gradual drying, the IA crystals after recrystallization were 99 % pure and the PR over the whole crystallization process was 78–80 %.

#### 4. Conclusions

Electrodialysis is a compatible and space saving technique that operated under normal temperature. In this study, an electro-dialytic process with a bipolar membrane was evaluated using model- and real fermentation effluents at elevated temperatures and different initial pHs. Based on the results, it is able to separate IA, and at the same time, has the ability for the colorants and glucose retainment. The side solutions could be reusable for the process control or the recirculation in the fermentation stage. It was observed that the combination of an elevated temperature with pH shifting by a NaOH solution intensified certain mass transport mechanisms during the EDBM process as well as resulted in significant water and IA transport from the Cacid to Cbase segment. Moreover, based on calculations, this caused a lower PR and CE under the same applied potential. The crystallization process was improved for the recovery of IA from the Cacid segment using the EDBM technique. Therefore, in contrast to the classical multistep downstream process, only one or two crystallization steps were required to produce pure IA. Based on these novel results, further experiments are planned to acquire data regarding the reusability of the residual diluate which is still rich in retained unmetabolized substrate. In conclusion, even though recent results have shown that the concept of a continuous fermentation-EDBM system coupled with crystallization is an emerging and promising method, further investigation is necessary to achieve more efficient IA production compared to classical multistep downstream processes.

#### CRedit authorship contribution statement

**Tamás Rózsenszki:** Investigation, Data curation, Formal analysis, Conceptualization, Visualization, Writing – original draft, Writing – review & editing, Supervision. **Péter Komáromy:** Investigation, Data curation, Formal analysis, Conceptualization, Writing – original draft, Writing – review & editing. **Éva Hülber-Beyer:** Investigation, Data curation, Conceptualization, Writing – original draft. **Andrea Pesti:** Investigation, Writing – original draft. **László Koók:** Investigation, Writing – original draft. **Péter Bakonyi:** Conceptualization, Supervision, Writing – review & editing. **Katalin Bélafi-Bakó:** Resources, Acquisition of funding, Project administration. **Nándor Nemestóthy:** Methodology, Resources, Supervision, Acquisition of funding, Project administration.

#### Declaration of Competing Interest

The authors declare that they have no known competing financial interests or personal relationships that could have appeared to influence the work reported in this paper.

#### Acknowledgements

This research was supported by the National Research, Development and Innovation Fund projects NKFIH OTKA K 119940 entitled “Study on the electrochemical effects of bioproduct separation by electrodialysis” and NKFIH-471-3/

2021 entitled “Establishment of a National Multidisciplinary Laboratory for Climate Change” financed by the Government of Hungary. Tamás Rózsenszki thanks for the support given by the János Bolyai Research Scholarship of the Hungarian Academy of Sciences.

## References

- Bafana, R., Pandey, R.A., 2018. New approaches for itaconic acid production: bottlenecks and possible remedies. *Crit. Rev. Biotechnol.* 38, 68–82. <https://doi.org/10.1080/07388551.2017.1312268>
- Dwiarti, L., Otsuka, M., Miura, S., Yaguchi, M., Okabe, M., 2007. Itaconic acid production using sago starch hydrolysate by *Aspergillus terreus* TN484-M1. *Bioresour. Technol.* 98, 3329–3337. <https://doi.org/10.1016/j.biortech.2006.03.016>
- Eggert, A., Maßmann, T., Kreyenschulte, D., Becker, M., Heyman, B., Büchs, J., Jupke, A., 2019. Integrated in-situ product removal process concept for itaconic acid by reactive extraction, pH-shift back extraction and purification by pH-shift crystallization. *Sep. Purif. Technol.* 215, 463–472. <https://doi.org/10.1016/j.seppur.2019.01.011>
- El-imam, A.A., Du, C., 2014. Biodiversity, bioprospecting and development. *J. Biodivers. Biopros Dev.* 1, 1–8.
- Erickson, B., Nelson, J.E., Winters, P., 2012. Perspective on opportunities in industrial biotechnology in renewable chemicals. *Biotechnol. J.* <https://doi.org/10.1002/biot.201100069>
- Gail Lorenz, M., 1959. Use of dinitrosaiicyic acid reagent for determination of reducing sugar. *Anal. Chem.* 31, 426–428.
- Gausmann, M., Kocks, C., Pastoors, J., Büchs, J., Wierckx, N., Jupke, A., 2021. Electrochemical pH-T-swing separation of itaconic acid for zero salt waste downstream processing. *ACS Sustain. Chem. Eng.* 9, 9336–9347. <https://doi.org/10.1021/acssuschemeng.1c02194>
- Geise, G.M., Hickner, M.A., Logan, B.E., 2013. Ionic resistance and permselectivity tradeoffs in anion exchange membranes. *ACS Appl. Mater. Interfaces* 5, 10294–10301. <https://doi.org/10.1021/am403207w>
- Gorden, J., Geiser, E., Wierckx, N., Blank, L.M., Zeiner, T., Brandenbusch, C., 2017. Integrated process development of a reactive extraction concept for itaconic acid and application to a real fermentation broth. *Eng. Life Sci.* 17, 809–816. <https://doi.org/10.1002/elsc.201600253>
- Handojo, L., Wardani, A.K., Regina, D., Bella, C., Kresnowati, M.T.A.P., Wenten, I.G., 2019. Electro-membrane processes for organic acid recovery. *RSC Adv.* 9, 7854–7869. <https://doi.org/10.1039/C8RA09227C>
- Kim, N., Jeon, J., Chen, R., Su, X., 2022. Electrochemical separation of organic acids and proteins for food and biomanufacturing. *Chem. Eng. Res. Des.* 178, 267–288. <https://doi.org/10.1016/j.cherd.2021.12.009>
- Klement, T., Büchs, J., 2013. Itaconic acid - a biotechnological process in change. *Bioresour. Technol.* 135, 422–431. <https://doi.org/10.1016/j.biortech.2012.11.141>
- Klement, T., Milker, S., Jäger, G., Grande, P.M., Domínguez de María, P., Büchs, J., 2012. Biomass pretreatment affects *Ustilago maydis* in producing itaconic acid. *Microb. Cell Fact.* 11. <https://doi.org/10.1186/1475-2859-11-43>
- Komáromy, P., Bakonyi, P., Kucska, A., Tóth, G., Gubicza, L., Bélafi-Bakó, K., Nemestóthy, N., 2019. Optimized pH and its control strategy lead to enhanced itaconic acid. *Ferment. Aspergillus Terre Glucose Substr. Ferment.* 5. <https://doi.org/10.3390/fermentation5020031>
- Komáromy, P., Rózsenszki, T., Bakonyi, P., Nemestóthy, N., Bélafi-bakó, K., 2020. Statistical analysis on the variables affecting itaconic acid separation by bipolar membrane electro dialysis. *Desalin. Water Treat.* 192, 408–414. <https://doi.org/10.5004/dwt.2020.25899>
- Kuenz, A., Gallenmüller, Y., Willke, T., Vorlop, K.D., 2012. Microbial production of itaconic acid: developing a stable platform for high product concentrations. *Appl. Microbiol. Biotechnol.* 96, 1209–1216. <https://doi.org/10.1007/s00253-012-4221-y>
- Kuenz, A., Krull, S., 2018. Biotechnological production of itaconic acid—things you have to know. *Appl. Microbiol. Biotechnol.* 102, 3901–3914. <https://doi.org/10.1007/s00253-018-8895-7>
- Lansing, J.C., Murray, R.E., Moser, B.R., 2017. Biobased methacrylic acid via selective catalytic decarboxylation of itaconic acid. *ACS Sustain. Chem. Eng.* 5, 3132–3140. <https://doi.org/10.1021/acssuschemeng.6b02926>
- López-Garzón, C.S., Straathof, A.J.J., 2014. Recovery of carboxylic acids produced by fermentation. *Biotechnol. Adv.* <https://doi.org/10.1016/j.biotechadv.2014.04.002>
- Magalhães, A.I., de Carvalho, J.C., Medina, J.D.C., Soccol, C.R., 2017. Downstream process development in biotechnological itaconic acid manufacturing. *Appl. Microbiol. Biotechnol.* 101. <https://doi.org/10.1007/s00253-016-7972-z>
- Magalhães, A.I., de Carvalho, J.C., Thoms, J.F., Medina, J.D.C., Soccol, C.R., 2019. Techno-economic analysis of downstream processes in itaconic acid production from fermentation broth. *J. Clean. Prod.* 206, 336–348. <https://doi.org/10.1016/j.jclepro.2018.09.204>
- Mahour, S., Kumar Verma, S., Kumar Arora, J., Srivastava, S., 2022. Carboxyl appended polymerized seed composite with controlled structural properties for enhanced heavy metal capture. *Sep. Purif. Technol.* 284, 120247. <https://doi.org/10.1016/j.seppur.2021.120247>
- Mikhaylin, S., Bazinet, L., 2016. Fouling on ion-exchange membranes: classification, characterization and strategies of prevention and control. *Adv. Colloid Interface Sci.* 229, 34–56. <https://doi.org/10.1016/j.cis.2015.12.006>
- Nagai, K., 2001. New developments in the production of methyl methacrylate. *Appl. Catal. A Gen.* 221, 367–377. [https://doi.org/10.1016/S0926-860X\(01\)00810-9](https://doi.org/10.1016/S0926-860X(01)00810-9)
- Narisetty, V., Prabhu, A.A., Al-Jaradah, K., Gopaliya, D., Hossain, A.H., Kumar Khare, S., Punt, P.J., Kumar, V., 2021. Microbial itaconic acid production from starchy food waste by newly isolated thermotolerant *Aspergillus terreus* strain. *Bioresour. Technol.* 337. <https://doi.org/10.1016/j.biortech.2021.125426>
- Nieder-Heitmann, M., Haigh, K.F., Görgens, J.F., 2018. Process design and economic analysis of a biorefinery co-producing itaconic acid and electricity from sugarcane bagasse and trash lignocelluloses. *Bioresour. Technol.* 262, 159–168. <https://doi.org/10.1016/j.biortech.2018.04.075>
- Okabe, M., Lies, D., Kanamasa, S., Park, E.Y., 2009. Biotechnological production of itaconic acid and its biosynthesis in *Aspergillus terreus*. *Appl. Microbiol. Biotechnol.* 84, 597–606. <https://doi.org/10.1007/s00253-009-2132-3>
- Pal, P., Kumar, R., Banerjee, S., 2016. Manufacture of gluconic acid: A review towards process intensification for green production. *Chem. Eng. Process. Process. Intensif.* <https://doi.org/10.1016/j.cep.2016.03.009>
- Regestein, L., Klement, T., Grande, P., Kreyenschulte, D., Heyman, B., Maßmann, T., Eggert, A., Sengpiel, R., Wang, Y., Wierckx, N., Blank, L.M., Spiess, A., Leitner, W., Bolm, C., Wessling, M., Jupke, A., Rosenbaum, M., Büchs, J., 2018. From beech wood to itaconic acid: Case study on biorefinery process integration. *Biotechnol. Biofuels.* <https://doi.org/10.1186/s13068-018-1273-y>
- Rózsenszki, T., Komáromy, P., Hülber-Beyer, É., Bakonyi, P., Nemestóthy, N., Bélafi-Bakó, K., 2021. Demonstration of bipolar membrane electrodialysis technique for itaconic acid recovery from real fermentation effluent of *Aspergillus terreus*. *Chem. Eng. Res. Des.* 175, 348–357. <https://doi.org/10.1016/j.cherd.2021.09.022>
- Rózsenszki, T., Komáromy, P., Korösi, E., Bakonyi, P., Nemestóthy, N., Bélafi-Bakó, K., 2020. Investigation of itaconic acid separation by operating a commercialized electrodialysis unit with bipolar membranes. *Processes* 8. <https://doi.org/10.3390/pr8091031>
- Saha, B.C., 2017. Emerging biotechnologies for production of itaconic acid and its applications as a platform chemical. *J. Ind. Microbiol. Biotechnol.* 44, 303–315. <https://doi.org/10.1007/s10295-016-1878-8>

- Strathmann, H., 2010. Electrodialysis, a mature technology with a multitude of new applications. *Desalination* 264, 268–288. <https://doi.org/10.1016/j.desal.2010.04.069>
- Sun, X., Lu, H., Wang, J., 2017. Recovery of citric acid from fermented liquid by bipolar membrane electrodialysis. *J. Clean. Prod.* 143, 250–256. <https://doi.org/10.1016/j.jclepro.2016.12.118>
- Szczygielda, M., Antczak, J., Prochaska, K., 2017. Separation and concentration of succinic acid from post-fermentation broth by bipolar membrane electrodialysis (EDBM). *Sep. Purif. Technol.* 181, 53–59. <https://doi.org/10.1016/j.seppur.2017.03.018>
- Tongwen, X., Weihua, Y., 2002. Citric acid production by electrodialysis with bipolar membranes. *Chem. Eng. Process.* 41, 519–524. [https://doi.org/10.1016/S0255-2701\(01\)00175-1](https://doi.org/10.1016/S0255-2701(01)00175-1)
- Tran, A.T.K., Mondal, P., Lin, J.Y., Meesschaert, B., Pinoy, L., Van der Bruggen, B., 2015. Simultaneous regeneration of inorganic acid and base from a metal washing step wastewater by bipolar membrane electrodialysis after pretreatment by crystallization in a fluidized pellet reactor. *J. Memb. Sci.* 473, 118–127. <https://doi.org/10.1016/j.memsci.2014.09.006>
- Wang, X., Wang, Y., Zhang, X., Feng, H., Xu, T., 2013. In-situ combination of fermentation and electrodialysis with bipolar membranes for the production of lactic acid: Continuous operation. *Bioresour. Technol.* 147, 442–448. <https://doi.org/10.1016/j.biortech.2013.08.045>
- Wu, X., Huang, X., Zhu, Y., Li, J., Hoffmann, M.R., 2020. Synthesis and application of superabsorbent polymer microspheres for rapid concentration and quantification of microbial pathogens in ambient water. *Sep. Purif. Technol.* 239, 116540. <https://doi.org/10.1016/j.seppur.2020.116540>
- Yahiro, K., Takahama, T., Park, Y.S., Okabe, M., 1995. Breeding of *Aspergillus terreus* mutant TN-484 for itaconic acid production with high yield. *J. Ferment. Bioeng.* 79, 506–508. [https://doi.org/10.1016/0922-338X\(95\)91272-7](https://doi.org/10.1016/0922-338X(95)91272-7)
- Yang, J., Xu, H., Jiang, J., Zhang, N., Xie, J., Zhao, J., Bu, Q., Wei, M., 2020. Itaconic acid production from undetoxified enzymatic hydrolysate of bamboo residues using *Aspergillus terreus*. *Bioresour. Technol.* 307. <https://doi.org/10.1016/j.biortech.2020.123208>
- Zambanini, T., Hosseinpour Tehrani, H., Geiser, E., Merker, D., Schleese, S., Krabbe, J., Buescher, J.M., Meurer, G., Wierckx, N., Blank, L.M., 2017. Efficient itaconic acid production from glycerol with *Ustilago vetiveriae* TZ1. *Biotechnol. Biofuels* 10. <https://doi.org/10.1186/s13068-017-0809-x>